the value of the diffusion coefficient uncertain.[9] As seen in Figure 4, all of the diffusion data are well represented by eq 9. However, since the effect of temperature on D is large, we have found that eq 7 also gives a good fit to the diffusion data. The fit gives a similar C_2 value when the same reference temperature is used. The WLF constants obtained are $C_1^D = 5.46$ and $C_2^D = 80.3$ K for the uncross-linked sample and $C_1^D = 8.70$ and $C_2^D = 83.7$ K for the 15% cross-linked sample.

The C_2^D value obtained by using eq 9 agrees, within experimental uncertainty, with that extracted from the shear creep data of atactic PMMA by Plazek et al.[10] (C_2 = 80 K). The value of C_1^D differs from the C_1 value obtained from the creep data[8] (C_1 = 14). This is expected, as the minimum void size in the sense of free-volume theory for the diffusant–polymer system is not the same in relation to the size of the moving unit underlying the creep experiment. The fact that $C_1^D/C_1 = 5.46/14 = 0.39$ is consistent with results of the comparison previously obtained.[4] In terms of the interpretation developed in ref 7, this ratio indicates that the size of CQ is only about 39% the volume of the polymer jumping unit. Note that, in contrast to the PS result, C_2^D for the cross-linked sample is less than of C_2^D in the uncross-linked polymer. Since there is a decrease in the thermal expansion coefficient of the cross-linked sample, the decrease in C_2^D for the cross-linked PMMA is apparently associated with the decrease of the free volume which outweights the decrease of thermal expansion coefficient.[4]

In summary, we have measured the diffusion coefficients of camphorquinone in linear PMMA and cross-linked PMMA. Over 0–50% (by weight) of the cross-linking agent concentration, the diffusion coefficient of CQ decreases drastically with increasing concentration of the cross-linking agent. The result can be satisfactorily interpreted in terms of free volume theory. The result of temperature-dependent studies is consistent with free volume theory. The diffusion coefficient appears to be insensitive to the molecular weight distribution. The WLF constants extracted from either plot are in agreement with those obtained from the viscoelastic data.

Acknowledgment. We thank the NSF Polymer Program (DMR 82-16221) and ONR for financial support. We also thank Z.-X. Chen for preparing the samples used in the optical measurement.

Registry No. CQ, 465-29-2; PMMA, 9011-14-7; (bisphenol A dimethacrylate)(MMA) (copolymer), 31547-90-7.

References and Notes

(1) Zhang, J.; Wang, C. H.; Chen, Z.-X. *J. Chem. Phys.* **1986**, *85*, 5359.
(2) Zhang, J.; Wang, C. H.; Ehlich, D. *Macromolecules* **1986**, *19*, 1390.
(3) Zhang, J.; Yu, B. K.; Wang, C. H. *J. Phys. Chem.* **1986**, *90*, 1299.
(4) Ferry, J. D. *Viscoelastic Properties of Polymers*, 3rd ed.; Wiley: New York, 1980.
(5) Zhang, J.; Wang, C. H. *J. Phys. Chem.* **1986**, *90*, 2296.
(6) Cohen, M. H.; Turnbull, D. *J. Chem. Phys.* **1959**, *31*, 1164.
(7) See, for example: Vrentas, J. S.; Duda, J. L.; Ling, H.-C. *J. Polym. Sci., Polym. Phys. Ed.* **1985**, *23*, 275. Vrentas, J. S.; Duda, J. L.; Ling, H.-C.; Hou, A.-C. *J. Polym. Sci., Polym. Phys. Ed.* **1985**, *23*, 289.
(8) Fujita, H. *Adv. Polym. Sci.* **1961**, *3*, 1.
(9) Zhang, J.; Wang, C. H. *Macromolecules*, in press.
(10) Plazek, D. J.; Tan, V.; O'Rourke, V. M. *Rheol. Acta* **1974**, *13*, 367.

Relaxation by Constraint Release in Combs and Star–Combs†

Jacques Roovers* and Paul M. Toporowski

Division of Chemistry, National Research Council of Canada, Ottawa, Ontario, Canada K1A 0R9. *Received December 19, 1986*

ABSTRACT: A number of polybutadiene combs and 4- and 18-arm star–combs have been prepared. They have been characterized by their dilute solution properties. The viscoelastic properties of their melts have been investigated over a wide range of frequencies and temperatures. The maximum in $G''(\omega)$ in the plateau zone has been correlated with a similar maximum in $G''(\omega)$ of regular stars and is attributed to the equilibration of the branches. The low-frequency behavior of $G''(\omega)$ and $G'(\omega)$ is Rouse-like. The experimental longest relaxation time (τ_1) depends exponentially on the branch length. Comparison of τ_1 for combs and star–combs suggests that τ_1 depends also on the square of the number of entanglements per backbone. These dependencies are consistent with relaxation of the backbone by constraint release.

Introduction

At least three classes of branched polymers are distinguished. Star polymers with a single branch point are the simplest. They are widely studied and have specific practical applications. Comb polymers have a linear backbone from which branches emanate. A large class of branched polymers have a randomly branched or treelike structure. They contain no clearly defined backbone and each branch in turn may carry branches.

In order to push the complexity of well-characterized branched polymers beyond that of comb polymers, star–combs have been prepared. Branches are grafted onto the arms of anionically prepared regular stars. The arms of the parent star and the branches have narrow MW distributions. The number of arms in the star (f) is fixed but the number of branches per molecule ($\bar{p}$) has a small distribution. The complexity of these polymers lies between that of combs and randomly branched polymers. Their architecture mimics to some extent the soft sphere polymers which have been described theoretically.[1] The polymer segments can be varied and are generally much looser and less regular than in the starburst-dendritic molecules.[2]

The synthesis and purification of polybutadiene star–combs are described. The polymers are characterized by their dilute solution properties. Some ordinary polybutadiene combs are included for comparison. Special

† Issued as NRCC No. 27823.

0024-9297/87/2220-2300$01.50/0 Published 1987 by the American Chemical Society

attention has been paid to the melt properties of the combs and star–combs.

The melt properties of combs[3-9] and randomly branched polymers[10-11] have been described, but their interpretation runs far behind that of star polymers.[12-17] The problem is outlined by the following argument. The zero-shear melt viscosity of stars is given by[16]

$$\eta_0 \propto N_a^{1/2} \exp(\nu N_a) \quad (1)$$

where N_a is the number of entanglements per arm and $\nu \approx 0.6$. For regular H-polymers (with two branch points) η_0 increases more rapidly approximately according to[18]

$$\eta_0 \propto N_a^{1/2} \exp(2\nu N_a) \quad (2)$$

A simple extension of eq 1 and 2 suggests that η_0 of combs with 20–30 branches would be immeasurably high except at very low N_{br} (number of entanglements per branch) in contrast with available data on combs.[3-9] A fortiori, the slow relaxation of the arms of a star is expected to be severely retarded by the branches in star–combs and, unless other mechanisms of relaxation are effective, star–combs will not exhibit measurable limiting properties. Any randomly branched polymer with many long segments would be similarly affected.[19]

Experimental Section

The star polybutadienes are prepared with *sec*-BuLi in benzene followed by coupling of the arms with 1,2-bis(methyldichlorosilyl)ethane[20] for 4-arm stars and $[(Cl_3SiCH_2CH_2)_3SiCH_2]_2$[21] for 18-arm stars. A small excess of CLi over SiCl bonds is used to ensure completion of the reaction. The resulting solution is freeze-dried under vacuum and the polymer dissolved in purified cyclohexane (1–2% solution) and lithiated with *sec*-BuLi–tetramethylethylenediamine (TMEDA) (1:1) complex for 2 h at room temperature.[22]

The branch polybutadiene of the star–combs is prepared separatedly with *sec*-BuLi in *n*-hexane. The living polymer solution is poured onto a 30-fold excess of $(CH_3)_2SiCl_2$ (DMDCS) in hexane at −20 °C. This produces polybutadiene with SiCl end groups and little dimerization. The solvent and excess DMDCS are removed without breaking the vacuum. The polymer is further dried with occassional slow stirring for 48 h at about 1 Pa and redissolved in cyclohexane.

The star–combs are formed on addition of the SiCl end-capped polybutadiene to the lithiated polybutadiene star and the mixture is left for 24 h. The excess branch material and some linear combs are first removed by fractionation in benzene–methanol. The star–comb is then refractionated. About 30% high and 20% low MW material are removed. The ordinary combs are made in the same way but the star-coupling reaction is omitted.

Molecular weights of the samples are determined by light scattering in cyclohexane at 25 °C (vertically polarized light; λ_0 = 436 nm; $dn/dc = 0.117_5$; Rayleigh ratio of benzene at 90° = 49 × 10^{-6}). Intrinsic viscosities are measured in toluene at 35 °C and in dioxane at 26.5 °C. It has been verified that the latter solvent is also a Θ solvent for the branched polybutadienes.[23] The number-average MW of some branch polymers has been determined by osmometry in toluene at 35 °C. These samples are then used to calibrate the size-exclusion chromatography (SEC) elution volume. The MW of the other branches has been measured by SEC. The microstructure of the polybutadienes prepared in benzene is 8–10% 1,2, 50% cis, and 40% trans as determined by ^1H and ^{13}C NMR. The branches prepared in *n*-hexane have 5% 1,2, 50% cis, and 45% trans units.

The melt properties have been measured with a Rheometrics mechanical spectrometer in the dynamic mode. The loss (G'') and storage (G') parts of the shear modulus are measured over a wide frequency ($1 \times 10^{-2} < \omega < 10^{-2}$ rad/s) and temperature range (106 to −75 °C). The master curves at the reference temperature (27 °C) are constructed by superposition of the data obtained at different temperatures with small vertical shifts, b_T, and horizontal shifts along the frequency axis (a_T). Details have been given previously.[24] The shift factors a_T and b_T are identical with those for 18-arm star polybutadienes.[25] The zero-shear viscosity is obtained from $\eta_0 = \lim_{\omega\to 0} (G''/\omega)$, the recoverable compliance $J_e^0 = (1/\eta_0^2) \lim_{\omega\to 0} (G'/\omega^2)$. The plateau modulus $G_N^0 = (2/\pi)\int_0^\infty (G'' - G''_s)\, d \ln \omega = 1.1 \times 10^7$ [17,25] dyn/cm^2 is independent of the architecture of the polymer. The molecular weight between entanglements $M_e = \rho RT/G_N^0 = 1970$ has been used.[17,25]

Table I
Characteristics and Dilute Solution Properties of Polybutadiene Star-Combs

sample	$M_w \times 10^{-5}$	$(M_n)_{br} \times 10^{-3}$	$\bar{p}$	$[\eta]_{Diox}^{26.2\,°C}$	$[\eta]_{Tol}^{35\,°C}$	Ψ
			Linear Combs			
backbone	0.50			0.45_2	0.76_2	
LC3B4	1.77_5	7.0_8	$17._9$	0.40_1	0.87	0.5_6
LC1B3	2.56	11.3	$18._1$	0.44_3	1.00	0.6_8
LC2B4	4.64	23.2	17.8	0.50_8	1.28	1.0
LC2T3	3.36	23.2	$12._3$			0.4_5
LC2B3	5.53	23.2	$21._7$			0.8_8
			4-Arm Star–Combs			
4SC1[a]	1.14_8			0.50_8	1.01_5	0.5_3
4SC3B3	2.18	5.2_5	$20._6$	0.45_5	1.04_5	0.7_4
4SC1T2	2.61	11.5	$13._4$	0.48_2	1.12	0.6_2
4SC1B3	3.10	11.5	$17._8$	0.47_7		0.6_6
4SC2B3	4.88	25.0	$15._7$	0.54_5	1.42_5	1.1
			18-Arm Star–Combs			
18SSCB2[b]	3.40			0.32_5	0.68_4	1.0
18SSC3B3	4.92	8.9_7	$17._0$	0.33_8	0.78_2	1.2
18SSC4B3	6.29	13.7	$21._0$	0.35_6	0.87	1.3
18SSC2B3	6.71	$27._0$	$12._3$	0.43_0	1.14	1.6
18SSC1B4	9.75	$25._8$	$24._6$	0.41_0	1.14	1.1

[a] Reference 17. [b] Reference 25.

Results and Discussion

Synthesis. The synthesis of the polybutadiene combs and star–combs is complex. The polybutadiene branches cannot be polymerized from the lithiated backbone because the resulting branches would have a predominantly 1,2 structure due to the presence of TMEDA. The reverse procedure in which the lithiated polybutadiene is treated with excess $(CH_3)_2SiCl_2$ leads to gelation. In a separate experiment it was established that the star structure is kept intact during lithiation.

The molecular characteristics of the combs and star–combs are given in Table I. The average number of branches per molecule, $\bar{p}$, is calculated from

$$\bar{p} = \frac{M_w - (M_w)_{bb}}{(M_n)_{br}} \quad (3)$$

where $(M_w)_{bb}$ is the weight-average molecular weight of the parent linear polymer of the combs or the parent star of the star–combs and $(M_n)_{br}$ is the number-average MW of the branch. Since the branching sites are fixed during lithiation, it can be assumed that the branches are randomly distributed along the parent polymer. The value of $\bar{p}$ is the average of a small distribution. The natural distribution has been narrowed further by fractionation. The values of $\bar{p}$ in Table I vary somewhat within each series due to the variable yield of the lithiation reaction.[22] In general, the 4-arm star–combs have $\bar{p}$ = 15, the 18-arm star–combs have $\bar{p}$ = 20, and the combs have $\bar{p}$ = 18. A few fractions with different $\bar{p}$ have been included in order to explore the dependence of properties on $\bar{p}$. Routine SEC indicates that the combs and star–combs studied are narrow molecular weight distribution type polymers.

Dilute Solution Properties. The dimensions of the present star–combs are too small to yield Θ-condition radii of gyration from light-scattering measurements. It is known, however, that Θ-solvent dimensions of polystyrene

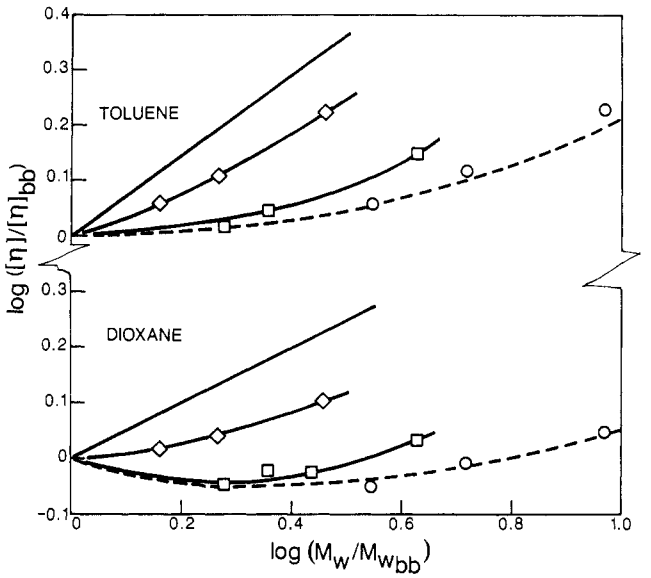

Figure 1. Intrinsic viscosities of combs and star-combs as a function of molecular weight relative to the parent backbone: (○) combs; (□) 4-arm star-combs; (◇) 18-arm star-combs; (straight line) $[\eta]$ for the homologous series of parent polymer; (broken line) comb polystyrenes.[26]

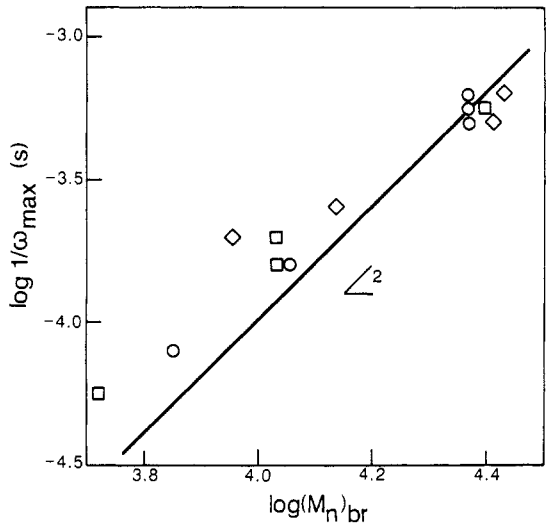

Figure 2. log-log plot of $1/\omega_{max} = T_{eq}$ vs. the molecular weight of the branches. Symbols as in Figure 1.

combs are larger than the random-walk prediction.[26] In cyclohexane, a good solvent, $\langle s^2 \rangle$ can be estimated and A_2 can be determined with good accuracy. The values of the noninterpenetration function[27]

$$\Psi = \frac{A_2 M^2}{4\pi^{3/2} N_A \langle s^2 \rangle^{3/2}} \qquad (4)$$

are given in Table I. It can be seen that Ψ increases with the number of arms and with the length of the branches. Values of Ψ for the 18-arm star-combs approach the hard-sphere limit (1.61). Similar observations have been made on polystyrene combs.[26]

The intrinsic viscosities of the star-combs are given in Table I and are plotted in Figure 1 as log $([\eta]/[\eta]_{bb})$ against log $(M_w/M_{w_{bb}})$. Plotted in this way, the data are less sensitive to small differences in $\bar{p}$. The relative increase of $[\eta]$ is most important in the 18-arm star-combs and least in the combs, showing the effect of the increased segment density in the parent polymer. In toluene $[\eta]$ increases more rapidly than in the Θ-solvent. Note that $[\eta]_\Theta$ of combs with small branches can be less than $[\eta]_\Theta$ of the

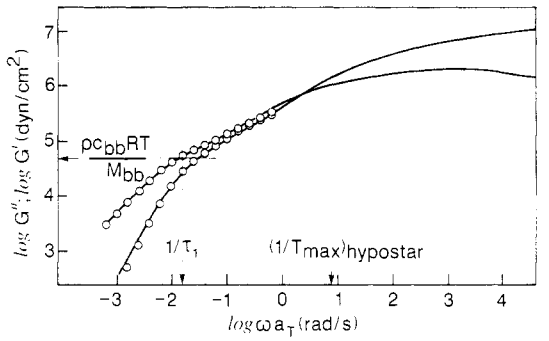

Figure 3. Moduli-frequency master curves for LC2B3; (circles) calculated for a terminal Rouse relaxation with eq 5 and 6. $(T_{max})_{hypostar}$: longest relaxation time for the hypothetical star with arm length equal to the branch length of the comb.

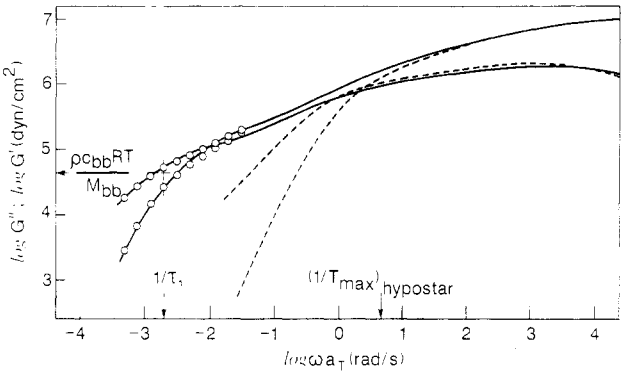

Figure 4. Moduli-frequency master curves for 4SC2B3 (solid lines). Circles: calculated for a terminal Rouse relaxation with eq 5 and 6. Broken lines: moduli-frequency curves of the parent backbone star.[17] $(T_{max})_{hypostar}$: longest relaxation time of the hypothetical star with arm length equal to branch length of the star-comb.

parent polymer.[8,26,28] The reduced $[\eta]$ data for the polybutadiene combs agree quite well with those for polystyrene combs with $\bar{p} = 29$.[26]

Melt Properties. Examples of the moduli-frequency behavior of combs and star-combs are shown in Figures 2–4. The enhancement of the moduli at low frequencies over those of the parent backbone (Figures 3 and 4) indicates that the combs and star-combs relax more slowly than their parent backbones. The combs and star-combs relax also more slowly than the hypothetical p-arm regular star with arm length equal to the length of the branches. The longest relaxation times of such stars can be calculated from those observed for 4-[17] and 18-arm[25] stars and are indicated as $(1/T_{max})_{hypostar}$ in Figures 2–4.

Three different types of entanglements should be distinguished in combs and star-combs.[5] Every backbone has $c_{bb}N_{bb}$ backbone–backbone entanglements, where $N_{bb} = (M_w)_{bb}/M_e$ and c_{bb} is the weight (or volume) fraction of the backbone in the sample, and $(1 - c_{bb})N_{bb}$ backbone–branch entanglements. The branch entanglements (N_{br}) are either branch–backbone ($c_{bb}N_{br}$ per branch) or branch–branch of which there are $(1 - c_{bb})N_{br}$ per branch. The mean-field distribution of backbones and branches is assumed.

The comb polymer backbones have two dangling ends which are better considered small branches. The effective number of entanglements per backbone is then approximately given by $N^*_{bb} = N_{bb}[1 - 2/(\bar{p} + 1)]$ and the effective weight fraction of the backbone is $c^*_{bb} = c_{bb}[1 - 2/(\bar{p} + 1)]$. For the star-combs the effective number of entanglements is given by $N^*_{bb} = N_{bb}[1 - 1/[(\bar{p}/f) + 1]]$ and $c^*_{bb} = c_{bb}[1 - 1[(\bar{p}/f) + 1]]$. The difference between N^*_{bb} and N_{bb} for the present linear combs and 4-arm star-combs is

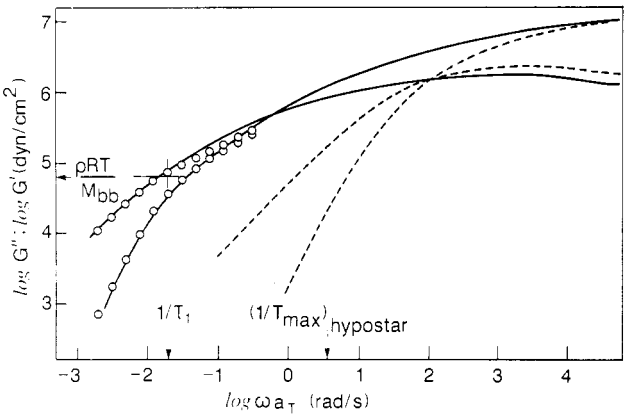

Figure 5. Moduli–frequency master curves for 18SSC1B4 (solid lines). Circles: calculated for a terminal Rouse relaxation with eq 8 and 9. Broken lines: moduli–frequency curves of the parent star.[25] $(T_{max})_{hypostar}$: longest relaxation time of the hypothetical star with arm length equal to the branch length of the star–comb.

small and can be neglected. However, in the case of the 18-arm star–combs N^*_{bb} and c^*_{bb} are considerably smaller than N_{bb} and c_{bb}, respectively.

From Figures 2–4 it can be seen that each $G''(\omega)$ curve has a maximum at a frequency ω_{max} in the plateau region. A double-logarithmic plot of $1/\omega_{max} = T_{eq}$ against $(M_n)_{br}$ is shown in Figure 5. T_{eq} increases with the square of $(M_n)_{br}$ and is practically equal to the contour-length equilibration time of 4-[17] and 18-arm[25] stars with arm molecular weights equal to $(M_n)_{br}$. The contour-length equilibration time of any tethered chain is therefore independent of the structure of the polymer to which the chain is attached, provided the monomeric friction coefficient is unchanged. Possible differences in the mean-square end-to-end distance of small branches may be responsible for their slightly larger T_{eq} as shown in Figure 5, although the differences are hardly outside the experimental accuracy. Note also that the smallest 18-arm star–comb has a large fraction of dangling arm segments whose equilibration occurs at a similar rate as the branches of the star–comb.

The complete relaxation of the branches of combs and star–combs is expected to proceed by the arm retraction mechanism proposed for stars,[12,14,15] although the process may extend to longer times than in stars due to the presence of branch–backbone entanglements. Relaxations of stars embedded in networks are known to be much slower than in the bulk, where constraint release is possible.[29] Diffusion measurements have also revealed the importance of the medium for the relaxation of stars.[30,31] As a first approximation branch–backbone entanglements can be considered permanent during the relaxation of the branches. However, contrary to entanglements in networks only a (small) fraction of entanglements of the branches is of the branch–backbone type. At present the effect of branch–backbone entanglements on the long time relaxation of the branches cannot be quantified. In practice, the contribution of branch relaxations to the moduli at frequencies between G''_{max} and the crossover frequency where $G''(\omega) = G'(\omega)$ (see Figures 2–4) cannot be estimated.

As shown in the introduction, reptation of the backbone of a comb and a fortiori the retraction of the arms of star–combs are unlikely mechanisms of relaxation, unless the branches are so small that they form no entanglements but act solely as diluent. However, the relaxation of the branches may be sufficient to induce the relaxation of the backbones. In that case, the relaxation of the backbone is possible by constraint release, a process in which the polymer segments can make lateral jumps whenever one

Table II
Melt Properties of Star–Combs at 300 K

sample	$M_w \times 10^5$	η_0, P	$J_e^0 \times 10^6$, cm²/dyn	log τ_1, s	log ω_{max}, s^{-1}
		Linear Combs			
backbone	0.5	3.6×10^4 [a]			
LC3B4	1.77_5	2.1×10^5	3.5	0.0	4.1
LC1B3	2.56	6.5×10^5	5.7	0.7	3.8
LC2B4	4.64	5.4×10^6	11	1.8	3.2_5
LC2T3	3.36	4.0×10^6	6	1.6	3.2
LC2B3	5.53	5.6×10^6	10	1.9	3.3
		4-Arm Star–Combs			
4SC1[b]	1.14_8	1.0×10^6	0.83		3.0
4SC3B3	2.18	1.5×10^6	2.5	0.6	4.2_5
4CS1T2	2.61	4.5×10^6	3.7	1.1	3.7
4SC1B3	3.10	5.3×10^6	5.0	1.2	3.8
4SC2B3	4.88	3.9×10^7	10	2.7	3.2_5
		18-Arm Star–Combs			
18SSCB2[c]	3.40	4.7×10^4	0.74		3.5_5
18SSC3B3	4.92	1.7×10^5	2.8	0.2	3.7
18SSC4B3	6.29	4.3×10^5	2.9	0.5	3.6
18SSC2B3	6.71	2.7×10^6	4.0	1.4	3.3
18SSC1B4	9.75	5.5×10^6	5.4	1.7	3.2

[a] Calculated with $\eta_0 = (4.7 \times 10^{-12})M_w^{3.38}$ from ref 41. [b] Reference 17. [c] Reference 25.

of its entanglements is temporarily abandoned.[15,32,33] A similar relaxation mechanism has been proposed very recently for the relaxation of randomly branched polystyrenes.[34] It is easiest to consider first the relaxation of combs and star–combs with **practically** isolated backbones, i.e., with almost no backbone–backbone entanglements. The terminal behavior of the combs and star–combs should conform to Rouse dynamics and[35]

$$G''(\omega) = \frac{\rho c_{bb} RT}{M_{bb}} \sum_{n=1}^{\infty} \frac{\omega \tau_n}{1 + \omega^2 \tau_n^2} \tag{5}$$

and

$$G'(\omega) = \frac{\rho c_{bb} RT}{M_{bb}} \sum_{n=1}^{\infty} \frac{\omega^2 \tau_n^2}{1 + \omega^2 \tau_n^2} \tag{6}$$

where $\tau_n = \tau_1/n^2$ and τ_1 is the longest relaxation time of the constraint release process. Note that $\rho c_{bb} N_A / M_{bb}$ corresponds to the number of backbone molecules per unit volume. Examples of the application of eq 5 and 6 are shown in Figures 2 and 3, where the fit is achieved by allowing τ_1 to vary. Experimental values of τ_1 are given in Table II.

The longest relaxation times for the constraint release process are expected to vary as[37]

$$\tau_1 \propto N^*_{bb}{}^2 T_{max} \tag{7}$$

When the backbone is a star as in the star–combs, N^*_{bb} is replaced by $((2/f)N^*_{bb})$ in eq 7, i.e., twice the number of entanglements per arm.[36-38] This would also slightly change the form of the terminal relaxation, but the difference with eq 5 and 6 is small. T_{max} in eq 7 is the longest relaxation time for the tube-forming material (the branches). As explained above, to a crude first approximation T_{max} can be equated with the longest relaxation time of a star with 4 or more arms with the same arm length as the branches. Since T_{max} of stars with $N_a \gg 1$ increases exponentially with N_a,[12-17] τ_1 is plotted exponentially against N_{br} in Figure 6. For comparison T_{max} of polybutadiene stars are also displayed.[25] Experimental values of τ_1 of the star–combs have been normalized to those of the linear comb backbone with $N^*_{bb} = 22.72$. The shift is given by a factor $(22.72/[(2/f)N^*_{bb}])^2$. This factor is not very large for the 4-arm star–combs (0.98) but im-

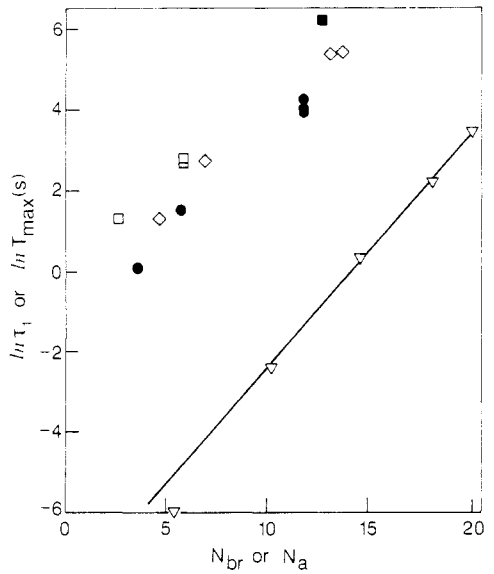

Figure 6. Exponential dependence of the longest relaxation times τ_1 normalized to constant N^*_{bb} against the molecular weight of the branches. Symbols as in Figure 1. Full symbols τ_1 by eq 5 and 6. Open symbols: τ_1 obtained by eq 8 and 9; (▽) T_{max} vs. N_a for four-arm star polybutadienes.[17]

portant for the 18-arm star–combs (4–8, depending on the value of $\bar{p}$ for each star–comb).

It is observed that the condition of the "isolated" backbone and the applicability of eq 5 and 6 are met when $c^*_{bb}M^*_{bb} < \rho M'_c$ where $M'_c \approx 7M_e$ and M_{bb} is replaced by $(2/f)M_{bb}$ for the star–combs. For combs with $c^*_{bb}M^*_{bb} > \rho M'_c$ the terminal moduli–frequency curves are well fitted to a Rouse relaxation by

$$G''(\omega) = \frac{\rho RT}{M_{bb}} \sum_{n=1}^{\infty} \frac{\omega\tau_n}{1 + \omega^2\tau_n^2} \tag{8}$$

and

$$G'(\omega) = \frac{\rho RT}{M_{bb}} \sum_{n=1}^{\infty} \frac{\omega^2\tau_n^2}{1 + \omega^2\tau_n^2} \tag{9}$$

which differ from eq 5 and 6 by a factor c_{bb}. An example is shown in Figure 4. In general, the frequency range over which eq 8 and 9 apply is small. Especially, at higher frequency $G''(\omega)$ increases above the prediction of eq 8 and relaxation of the branches in the plateau zone interferes. Experimental values of τ_1 are given in Table II and values of τ_1 normalized to the backbone of the linear combs are also plotted in Figure 6.

Note that the slopes of τ_1 and T_{max} in Figure 6 are very similar. This supports the assumption that the longest relaxation process of the combs and star–combs is dominated by the relaxation of the branches. There is no direct evidence that τ_1 is proportional to $N^*_{bb}{}^2$. However, the normalization of the star–combs to the combs by $(22.72/[(2/f)N^*_{bb}])^2$ is in agreement with a $N_{bb}{}^2$ dependence. The experimental ratio τ_1/T_{max} for the combs is roughly equal to $N^*_{bb}{}^2$. It is almost certainly fortuitous that the numerical coefficient in eq 7 is about unity. It is in contrast with smaller factors (≈0.1) from estimates of constraint release times in linear matrices.[38-40] The numerical coefficient in eq 7 is obtained on the assumption that T_{max} of stars applies. Any retardation of the relaxation of the branches compared to the arms in a star reduces this coefficient. In Figure 6 it can be seen that the reduced τ_1 values for the star–combs are systematically somewhat larger than for the combs. This may be due to the presence of branch–backbone entanglements on the branches. Indeed in the combs each branch has on average one branch–backbone entanglement but in the star–combs each branch has on average two branch–backbone entanglements. The branches in the star–combs are therefore expected to relax somewhat slower than in the combs.

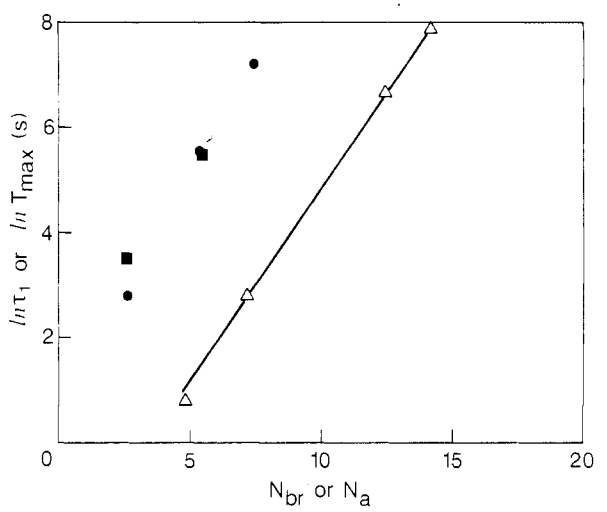

Figure 7. Exponential dependence of the longest relaxation times τ_1 normalized to constant N_{bb} against the molecular weight of the branches: (□) combs C642 and C652; (○) H-shaped polystyrenes; full symbols for τ_1 based on eq 5 and 6; (△) T_{max} of 4-arm star polystyrenes.[17]

Equations 5 and 6 can also be applied successfully to two polystyrene combs C652 and C642.[9] The other combs in that series do not have $N_{br} > 1$. Similarly, the moduli–frequency curves of large H-shaped polystyrenes show also a Rouse-like terminal behavior[18] and eq 5 and 6 with $c_{bb} = c^*_{bb} = 0.20$ can be applied. The τ_1 values normalized by a $N_{bb}{}^2$ dependence to $N_{bb} = 7.5$ of the H3A1A H-polymer[18] are shown in Figure 7 and compared with T_{max} of 4-arm polystyrene stars. Note that the range of N_{br} is smaller for the polystyrenes than for the polybutadienes. This obviously precluded a correct analysis.[9] The ratio $\tau_1/T_{max} \approx N_{bb}{}^2$ as for polybutadiene combs.

In so far as the zero-shear viscosity of the combs and star–combs is dominated by the longest relaxation time, η_0 is expected to scale as τ_1. Indeed a plot of ln η_0 (see Table II) against N_{br} has the same features as τ_1 in Figure 6.

The zero-shear recoverable compliance of the combs and the star–combs is plotted against M_w in Figure 8. It can be seen that in the series of linear combs J_e^0 increases from the pure backbone value[41] according to $(M_w/M_{bb})^2 \equiv c_{bb}{}^{-2}$. This has been observed previously for polystyrene combs and has been shown in a reduced form in Figure 9 of ref 9. The $c_{bb}{}^{-2}$ dependence of J_e^0 is identical with that for a entangled linear polymer diluted with low MW polymer.[17] In Figure 8, the $c_{bb}{}^{-2}$ dependence of J_e^0 changes to a $c_{bb}{}^{-1}$ dependence when the branches of the combs are very long and $c_{bb}M_{bb} < \rho M'_c \approx 7M_e$. The same transition has been more clearly established previously for the polystyrene combs.[9] The $c_{bb}{}^{-1}$ dependence is Rouse-like and is consistent with the fact that the backbones of these combs have few mutual entanglements.

The behavior of J_e^0 of the 4-arm star–combs is similar to that of the linear combs with a transition from $c_{bb}{}^{-2}$ to $c_{bb}{}^{-1}$ dependence when the branches become long. The J_e^0 values of the 18-arm star–combs are all in the $c_{bb}{}^{-2}$ region, in agreement with the observed terminal moduli behavior.

Conclusion

The combs and star–combs were prepared primarily for the exploration of their melt properties. The dimensions

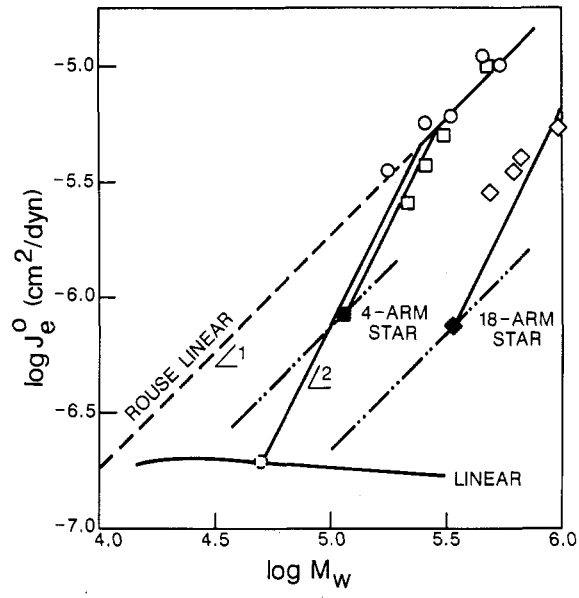

Figure 8. log–log plot of the zero-shear recoverable compliance of combs and star–combs as a function of molecular weight. Symbols as in Figure 1. The solid points are for the backbones. The broken line is for the theoretical Rouse model of linear polymers. The chain lines are for 4- and 18-arm stars.[17,25]

of the polymers are too small to be determined by light scattering in a Θ-solvent. The data obtained in a good solvent are in agreement with those previously observed for polystyrene combs.[26] It is therefore likely that the Θ-solvent expansion found for polystyrene combs[26] and 18-arm stars[25] is a general feature of all highly branched polymers. The chain expansion seems not to affect G_N^0 nor M_e, however.

It has been shown that the relaxation of combs and star–combs involves two processes. At short times the branches equilibrate their contour-length and relax thereafter by the retraction mechanism known for the relaxation of the arms of regular stars. The presence of branch–backbone entanglement may retard the final relaxation of the branches compared to the arm with the same length in a star melt. It is proposed that the relaxation of the effective backbone, i.e., all the segments of the branched polymer between two branch points, occurs by constraint release, the constraints being mostly of the type backbone–branch. It is shown that the terminal behavior is Rouse-like in agreement with a dominant constraint release relaxation mechanism. The longest relaxation times depend exponentially on the branch length. For experimental reasons this length is still small, however, and an extension to higher branch length would be desirable. Although no direct evidence is available for a longest time dependence of the form $\tau_1 \propto N^*_{bb}{}^2$, the relaxation times of combs and 4- and 18-arm star–combs are consistent with such dependence. Also, the longest relaxation times of polystyrene combs with $p = 29$ and H combs can be reduced by assuming the $N^*_{bb}{}^2$ dependence.

Relaxation by constraint release leads directly to an understanding of the weak dependence of η_0 on the number of branches in the comb.[5] A similar weak dependence on the number of branches can be seen for values of τ_1 in Table II. Indeed, by keeping the backbone and branches constant the major parameters affecting constraint release are kept unchanged. An increase in the number of branches increases N^*_{bb} slightly.

It would be interesting to apply the same analysis to randomly branched polymers, e.g., to the recently published results.[34] Such analysis will require the introduction of some distribution of branches to characterize the tube-forming material. The concept of the longest path through a randomly branched polymer[42] may be relevant to the length of the tube that is subject to relaxation by constraint release.

Finally it is worthwhile to note that constraint release plays a dominant role in the terminal relaxation of polymers whenever there are relaxation processes with widely different time scales. This is now well studied for binary mixtures of linear polymers[39,43] and for stars in linear polymers.[38] In combs the necessary wide range of relaxation times are built into each molecule. In melts of regular stars constraint release may be competing effectively with relaxation by arm retraction.[44]

Acknowledgment. J.R. profited greatly from a discussion with R. Colby and M. Rubinstein.

Registry No. Polybutadiene, 9003-17-2; (1,2-bis(methyldichlorosilyl)ethane)(butadiene) (copolymer), 109011-03-2; (butadiene)(($(Cl_3SiCH_2CH_2)_3SiCH_2)_2$) (copolymer), 108968-94-1.

References and Notes

(1) Burchard, W. *Adv. Polym. Sci.* **1983**, *48*, 1.
(2) Tomalia, D. A.; et al. *Polym. J.* **1985**, *17*, 117.
(3) Long, V. C.; Berry, G. C.; Hobbs, L. M. *Polymer* **1964**, *5*, 517.
(4) Berry, G. C.; Fox, T. G. *Adv. Polym. Sci.* **1968**, *5*, 261.
(5) Fujimoto, T.; Narukawa, H.; Nagasawa, M. *Macromolecules* **1970**, *3*, 57.
(6) Fujimoto, T.; Kajiura, H.; Hirose, M.; Nagasawa, M. *Polym. J.* **1972**, *3*, 181.
(7) Isono, Y.; Fujimoto, T.; Kajiura, H.; Nagasawa, M. *Polym. J.* **1980**, *12*, 369.
(8) Pannell, J. *Polymer* **1972**, *13*, 2.
(9) Roovers, J.; Graessley, W. W. *Macromolecules* **1981**, *14*, 766.
(10) Graessley, W. W.; Prentice, J. S. *J. Polym. Sci., Polym. Phys. Ed.* **1968**, *6*, 1887.
(11) Masuda, T.; Nakagawa, Y.; Ohta, Y.; Onogi, S. *Polym. J.* **1972**, *3*, 92.
(12) de Gennes, P.-G. *J. Phys. (Paris)* **1975**, *36*, 1199.
(13) Roovers, J.; Graessley, W. W. *Macromolecules* **1979**, *12*, 959.
(14) Doi, M.; Kuzuu, N. Y. *J. Polym. Sci., Polym. Lett. Ed.* **1980**, *18*, 775.
(15) Graessley, W. W. *Adv. Polym. Sci.* **1982**, *47*, 67.
(16) Pearson, D. S.; Helfand, E. *Macromolecules* **1984**, *17*, 888.
(17) Roovers, J. *Polymer* **1985**, *26*, 1091.
(18) Roovers, J. *Macromolecules* **1984**, *17*, 1196.
(19) Graessley, W. W. *Acc. Chem. Res.* **1977**, *10*, 332.
(20) Roovers, J.; Bywater, S. *Macromolecules* **1972**, *5*, 384.
(21) Hadjichristidis, N.; Fetters, L. J. *Macromolecules* **1980**, *13*, 191.
(22) Roovers, J.; Hadjichristidis, N. *J. Polym. Sci., Polym. Phys. Ed.* **1978**, *16*, 851.
(23) Hadjichristidis, N.; Zhongde, X.; Fetters, L. J.; Roovers, J. *J. Polym. Sci., Polym. Phys. Ed.* **1982**, *20*, 743.
(24) Hadjichristidis, N.; Roovers, J. *Polymer* **1985**, *26*, 1087.
(25) Roovers, J.; Toporowski, P. M. *J. Polym. Sci., Polym. Chem. Ed.* **1986**, *24*, 3009.
(26) Roovers, J. *Polymer* **1979**, *20*, 843.
(27) Yamakawa, H. *Modern Theory of Polymer Solutions*; Harper and Row: New York, 1971.
(28) Pannell, J. *Polymer* **1971**, *12*, 558.
(29) Kan, H.-C.; Ferry, J. D.; Fetters, L. J. *Macromolecules* **1980**, *13*, 1571.
(30) Klein, J.; Fletcher, D.; Fetters, L. J. *Faraday Symp. Chem. Soc.* **1983**, *18*, 159.
(31) Bartels, C. R.; Crist, B.; Fetters, L. J.; Graessley, W. W. *Macromolecules* **1986**, *19*, 785.
(32) Klein, J. *Macromolecules* **1978**, *11*, 852.
(33) Daoud, M.; de Gennes, P.-G. *J. Polym. Sci., Polym. Phys. Ed.* **1979**, *17*, 1971.
(34) Masuda, T.; Ohta, Y.; Onogi, S. *Macromolecules* **1986**, *19*, 2524.
(35) Rouse, P. E. *J. Chem. Phys.* **1953**, *21*, 272.
(36) Zimm, B. H.; Kilb, R. W. *J. Polym. Sci.* **1959**, *37*, 19.
(37) Klein, J. *Macromolecules* **1986**, *19*, 105.
(38) Roovers, J. *Macromolecules* **1987**, *20*, 148.

(39) Monfort, J. P.; Marin, G.; Monge, P. *Macromolecules* **1984**, *17*, 1551.
(40) Green, P. F.; Mills, P. J.; Palmstrom, C. J.; Mayer, J. W.; Kramer, E. J. *Phys. Rev. Lett.* **1984**, *53*, 2145.
(41) Roovers, J. *Polym. J.* **1986**, *18*, 153.
(42) Miller, D. R.; Valles, E. M.; Macosko, C. W. *Polym. Eng. Sci.* **1979**, *19*, 272.
(43) Struglinski, M. J.; Graessley, W. W. *Macromolecules* **1985**, *18*, 2630; **1986**, *19*, 1754.
(44) Pearson, D. S., private communication.

Notes

Peptide Synthesis by Fragment Condensation on a Soluble Polymer Support. 8.[1] Maximum Peptide Chain Lengths of Carboxyl Component Peptides for Effective Coupling Reactions with Amino Component Peptides Anchored to Soluble and Cross-Linked Polystyrene Supports

MITSUAKI NARITA,* SHIZUKO ISOKAWA, SATOSHI NAGASAWA, and TAKUYA ISHIJIMA

Department of Industrial Chemistry, Faculty of Technology, Tokyo University of Agriculture and Technology, Koganei, Tokyo 184, Japan. *Received December 2, 1986*

Peptide synthesis by fragment condensation on a polymer support has been thought to be one of the most promising methods for synthesizing large peptides and proteins.[2] However, one serious problem of the method is, as often observed, its low yields in fragment condensation reactions on cross-linked resin supports. It is believed that the problem results from the restricted permeability of carboxyl component peptides into resin matrices.[2-4] In addition, it has been demonstrated that a 1%-cross-linked polystyrene support commonly used in solid-phase peptide synthesis is sufficiently flexible for interactions among pendant functional groups.[5-7] The onset of a β-sheet aggregation by hydrogen bonding among pendant peptide chains brings about additional cross-linking of the polymer network.[5] In this case, the coupling efficiencies of carboxyl component peptides with pendant peptides were remarkably decreased as the carboxyl component peptide chain is lengthened.[3] On the other hand, we proposed a few strategies for solubility improvement of peptides in which the peptides are forced not to adopt a β-sheet structure.[8-10] As previously proposed,[3] we believe that the combination of these strategies and fragment condensation on a soluble polymer support has promising versatility for syntheses of pure large peptides and proteins.

This paper investigates the effect of peptide chain length of carboxyl component peptides on the coupling yields in the reactions with amino component peptides anchored to soluble polystyrene, and poly(styrene-*co*-1% (and -2%) divinylbenzenes). In the fragment condensation on a polymer support, it is better to use as large a peptide fragment as possible in order to obtain a pure product by simple purification procedures. This study elucidates the maximum chain lengths of carboxyl component peptides for effective coupling reactions with amino component peptides on polymer supports. In the reactions, the carboxyl components should be free from a β-sheet aggregation to evaluate the maximum peptide chain length. All of the carboxyl component peptides used in this study were previously synthesized to ascertain that the concept of "peptide segment separation" is useful as one of the strategies to improve solubility and to show their structures are predominantly in a randomly coiled structure in polar solvents.[9,11]

Experimental Section

Materials. The soluble H-$(\beta\text{-Ala})_2$-*p*-(oxymethyl)phenylacetamidomethylated polystyrene A (amino content, 39 μmol/g) was prepared from Boc-$(\beta\text{-Ala})_2$-*p*-(oxymethyl)phenylacetic acid and aminomethylated polystyrene by the method described previously.[12,13] The soluble H-$(Phe)_3$-*p*-(oxymethyl)phenylacetamidomethylated polystyrene B (amino content, 19 μmol/g) was prepared by copolymerization of styrene (99.6 mol %), Boc-Phe_3-(oxymethyl)phenylacetamidomethylated styrene (0.2 mol %), and divinylbenzene (0.2 mol %) followed by deprotection of the Boc group as described previously.[13] Poly(styrene-*co*-1% (and -2%) divinylbenzene) beads of 200-400 mesh, Bio-Beads S-X1 and S-X2, were purchased from Bio-Rad Laboratories. They were aminomethylated as described in the literature,[12] coupled with Boc-$(\beta\text{-Ala})_3$-*p*-(oxymethyl)phenylacetic acid and deprotected to give cross-linked H-$(\beta\text{-Ala})_3$-*p*-(oxymethyl)phenylacetamidomethylated polystyrene C (cross-linked with 1% divinylbenzene) and D (cross-linked with 2% divinylbenzene), respectively.

The large carboxyl component peptides, Boc-$(Leu_3Pro_2Gly)_n$-OH (n = 1, 2, 4, 6, 8, 10, 12; the peptides 1-7) were those previously prepared.[9]

General Method of Coupling Reactions of Boc-peptides 1-7 with the Peptides on the Polymer Supports A-D. To the solution of each Boc-peptide (10 equiv) in *N*-methylpyrrolidone (NMP) or in NMP/CH_2Cl_2 (volume ratio 1/1) (1 mL), each of the amino component peptide polymers A, C, or D (100 mg) was added. Then, HOBt (10 equiv) in the solvent (0.5 mL) and DCC (10 equiv) in the solvent (0.5 mL) were added to the reaction mixture, and it was stirred for 2 days at room temperature. When using the soluble peptide polymer A, the reaction mixture was poured into ethanol (20 mL) with stirring. The precipitated peptide polymer was filtered off, washed with ethanol, and dried in vacuo at 50 °C. When using the cross-linked peptide polymer C or D, the mixture was filtered off and the residue was washed with ethanol and dried in vacuo at 50 °C. Each resulting peptide polymer was subjected to acid hydrolysis and then to amino acid analysis. Coupling yield was obtained from the ratio of each corresponding peptide content and the β-Ala content of the peptide polymer.

When using the peptide polymer B, 4 equiv each of Boc-peptide, HOBt, and DCC was used and coupling reactions were carried out in NMP for 5 days at room temperature.

Results and Discussion

It has already been established that the carboxyl component peptides 1-7 used here have a randomly coiled structure in highly polar solvents such as NMP,[9,11] and it is also expected that the peptides have a predominantly randomly coiled structure in NMP/CH_2Cl_2. It has also been suggested by NMR studies that the carboxyl component sequential polypeptides have a repeating local conformation characteristic of the internal hexapeptide segment $Pro_2GlyLeu_3$, and the N-terminal Leu_3 and C-terminal Pro_2Gly segments have local conformations common to the sequential polypeptides in polar solvents.[11] Therefore, it is expected that only the effect of peptide

0024-9297/87/2220-2306$01.50/0